Electron Localization and the Second Moment of the Exchange Hole

J. G. ÁNGYÁN

Équipe Modélisation Quantique et Cristallographique, CR2M, UMR 7036, Institut Jean Barriol, Nancy-University, CNRS, B.P. 239, F-54506, Vandœuvre-lès-Nancy, France

ABSTRACT: The localization tensor, which is a global measure of the itinerant character of the electrons, has been defined by Resta as the second cumulant moment of the position operator per electron. It seems to be a meaningful parameter not only for solids but also for finite molecular systems. In the independent-particle limit, this quantity can be interpreted as the density-weighted average of the second moment of the exchange hole. After examining several possible local measures based on the moment analysis of the exchange hole, it turns out that the density weighted squared exchange hole dipole moment might be a useful local indicator of electron localization. © 2009 Wiley Periodicals, Inc. Int J Quantum Chem 109: 2340–2347, 2009

Key words: electron localization; Fermi-hole; ELF

1. Introduction

The characterization of electron localization and delocalization, or in other terms, of nonitinerant or itinerant nature of electrons, is of paramount importance for the understanding of physical and chemical properties of molecules and solids. While the study of the electron density provides precious pieces of information about the static distribution of the electronic charge in three-dimensional space, [1] the problem of localization/delocalization concerns mainly the mobility of electrons, i.e., their propensity to respond to an external perturbation. The insulating and conducting states of solid matter provides the paradigm of localized or nonitinerant and delocalized or itinerant character of electrons, respectively [2]. While in the realm of small molecular systems it is obviously of not too much sense to speak about "conducting" or "insulating" properties, one can nevertheless observe analogous trends in the organization of electrons in the molecular world as well [3]. The overall mobility of electrons on a given molecular frame influences their spectroscopic and physicochemical properties and it is an essential parameter to understand chemical reactivity.

The description of localization properties has followed quite different pathways in solid state physics [4] and quantum chemistry [5] communities. However, by the virtue of some new concepts emerged on the both sides, it became possible to close the gap between chemists' and physicists' viewpoints, which previously seemed to be quite divergent. A significant step in this direction is due to Resta, who reformulated Kohn's theory of insulating state in terms of the properties of the localization tensor, defined by the second cumulant moment of the electronic position operator. [6] It has been shown [3] that the quantum chemical localization criterion of Boys [7, 8], formulated as the minimum of the total quadratic spread of the one-electron orbitals, is closely related to the localization tensor. In particular, in a conducting state of a large cluster the quadratic spread, similar to the trace of the localization tensor, diverges with increasing system dimensions [3].

Another, viewpoint is represented by the electron localization function (ELF) [9], and other related functions which, in contrast to the global criterion provided by the localization tensor, provide a point-wise characterization of the localized or delocalized nature of electrons in both molecules and solids. There are several, complementary physical interpretations of ELF, e.g., as the local curvature of the exchange-hole [10], or as the excess kinetic energy density due to the Pauli-principle [11]. The ELF lends itself to a topological analysis [12], leading to a partition of the three-dimensional space to a set of domains, each attributed to an electron pair. A classification of attractors and basins of the ELF gradient field and an analysis of their relationships allows one to have a rigorous definition of various types of bonds, lone pairs, etc. [13]. There are numerous alternative variants of pointwise measures of electron localization. An ELF-like function based on the analysis of spin-pair concentrations has been defined by Silvi [14]. This idea has been generalized in the form of the ELI (electron localizability indicator) [15, 16]. The LOL (localized orbital locator) is a functional of the positive definite kinetic energy density [17], leading also to ELF-like pictures of the electron localization. A common feature of these electron localization measures is that they are constructed from local derivative and local kinetic energy density information, related to the Taylor expansion of the exchange hole. A somewhat different philosophy consists in taking various partially averaged forms of the exchange or exchange-correlation pair densities, which seem to provide interesting insights in the organization of electrons, as exemplified by the recent work of Geier [18].

A third technique, which lies between the global characterization of the electron localization and their local measures, consists in the study of the fluctuation of population between appropriately defined domains. Such domains can be defined according to various criteria. The physical space can be partitioned into nonoverlapping domains, like in the QTAIM approach [1] or to fuzzy, overlapping domains, like in the Hirschfeld-type partitioning schemes [19]. Alternatively, in the framework of LCAO, the partitioning can be performed directly on the set of basis functions, which are assigned to atomic centers [20]. The fluctuation of the atomic populations between pairs of atomic domains, defined in one of the partitioning schemes, provides various measures of delocalization. These quantities can also be assimilated to the notion of covalent bond orders or covalent bond indices [21]. It is to be noted that there is a correlation between the preferred pathways of charge flow between atoms [22], as measured by their charge-flow polarizabilities [23, 24], and the covalent bond orders [21, 25–27], which have also been interpreted as delocalization [28] or shared-electron distribution [29] indices.

A closer scrutiny of these approaches reveals that the central quantity is the exchange-correlation part of pair-density of the electrons, most often used in the form of the exchange-correlation hole, usually limited to its exchange component, the Fermi-hole [30]. In fact, the Fermi-hole (or exchange-hole, x-hole) establishes a link between apparently quite different notions like the localized orbitals and the electron density fluctuation. On the one hand, it is known that the shape x-hole is approximately equal to the negative of the density of a localized orbital, while on the other hand the dominant contribution to the charge density fluctuations is due to the Fermi-correlations, characterized by the x-hole. This relationship has been exploited, e.g., in the domain-averaged Fermi-hole approach of Ponec [31]. The connection between the fluctuation of electron density or of the population in a given region and various forms of the ELF has been analyzed recently by Ayers [32]. A stimulating discussion of the connection between fluctuation and localization, focusing on the role of electron correlation, can be found in the article of Ziesche [33].

The aforementioned approaches are just some examples from the panoply of tools and measures available for a characterization of electron localization and delocalization. To obtain a full insight, it is often recommended to use them in a

complementary manner. As to my knowledge, it has never been attempted to identify a local measure of electron localization, which would be directly connected to the localization tensor of Resta, or more precisely to its trace. The main purpose of this work is to explore some alternative possibilities to define a useful local measure electron localization, which is able to provide information about the itinerant or nonitinerant character of electrons in a pointwise manner in the three-dimensional space and which is based on the spatial extension of the exchange (or exchange-correlation) hole belonging to each particular point in the space.

In the next section, the localization tensor is introduced and its relationship to the xc-hole is discussed. Section 3 overviews possible proposals for a local measure of electron localization, illustrated by a few simple molecular systems in Section 4, followed by some conclusions and perspectives in Section 5.

2. Localization Tensor of Resta

The localization tensor has been defined [6] as $(1/N)\langle\hat{r}_\alpha\hat{r}_\beta\rangle_c$, i.e., as the second cumulant moment of the electron distribution,

$$\langle\hat{r}_\alpha\hat{r}_\beta\rangle_c = \left\langle\Psi\left|\sum_{i,j=1}^{N}\hat{r}_\alpha(i)\hat{r}_\beta(j)\right|\Psi\right\rangle$$
$$- \left\langle\Psi\left|\sum_{i=1}^{N}\hat{r}_\alpha(i)\right|\Psi\right\rangle\left\langle\Psi\left|\sum_{j=1}^{N}\hat{r}_\beta(j)\right|\Psi\right\rangle, \quad (2.1)$$

normalized by the number of electrons N. Here Ψ is the N-electron wave function and $\hat{r}_\alpha(i)$ is the $\alpha = x,y,z$ component of the i-th electronic position vector. Throughout this article, for the sake of notational simplicity, the second cumulant moment will be considered as the central quantity. Taking the electron density operator, $\hat{\rho}(\boldsymbol{r}) = \sum_i\delta(\boldsymbol{r} - \boldsymbol{r}_i)$, the electronic position operator can be written as $\sum_i\hat{r}_\alpha(i) = \int d\boldsymbol{r}r_\alpha\hat{\rho}(\boldsymbol{r})$ and we obtain the second cumulant moment as

$$\langle\hat{r}_\alpha\hat{r}_\beta\rangle_c = \iint d\boldsymbol{r}d\boldsymbol{r}'r_\alpha r'_\beta S(\boldsymbol{r},\boldsymbol{r}'). \quad (2.2)$$

Here, the density autocorrelation function, or form factor [34], $S(\boldsymbol{r},\boldsymbol{r}')$, is defined as

$$S(\boldsymbol{r},\boldsymbol{r}') = \langle\Psi|\hat{\rho}(\boldsymbol{r})\hat{\rho}(\boldsymbol{r}')|\Psi\rangle - \langle\Psi|\hat{\rho}(\boldsymbol{r})|\Psi\rangle\langle\Psi|\hat{\rho}(\boldsymbol{r}')|\Psi\rangle.$$
$$(2.3)$$

The form factor is symmetric in its variables, $S(\boldsymbol{r},\boldsymbol{r}') = S(\boldsymbol{r}',\boldsymbol{r})$, and satisfies the charge conservation sum rule, $\int d\boldsymbol{r}'S(\boldsymbol{r},\boldsymbol{r}') = 0$. It can be expressed by the exchange-correlation-hole, $h_{xc}(\boldsymbol{r},\boldsymbol{r}')$ as

$$S(\boldsymbol{r},\boldsymbol{r}') = \rho(\boldsymbol{r})\delta(\boldsymbol{r} - \boldsymbol{r}') + \rho(\boldsymbol{r})h_{xc}(\boldsymbol{r},\boldsymbol{r}'), \quad (2.4)$$

where $h_{xc}(\boldsymbol{r},\boldsymbol{r}')$ is given by the pair-density of electrons, $P_2(\boldsymbol{r},\boldsymbol{r}')$ as

$$\rho(\boldsymbol{r})h_{xc}(\boldsymbol{r},\boldsymbol{r}') = P_2(\boldsymbol{r},\boldsymbol{r}') - \rho(\boldsymbol{r})\rho(\boldsymbol{r}'). \quad (2.5)$$

By the virtue of the zero-temperature fluctuation-dissipation theorem, the following relationship holds between the form factor $S(\boldsymbol{r},\boldsymbol{r}')$ and the imaginary part of the frequency-dependent charge density response function, $\chi(\boldsymbol{r},\boldsymbol{r}';\omega)$:

$$S(\boldsymbol{r},\boldsymbol{r}') = \frac{\hbar}{\pi}\int_0^\infty d\omega\chi(\boldsymbol{r},\boldsymbol{r}';i\omega). \quad (2.6)$$

By consequence, the second cumulant moment is related to the frequency-dependent dipole polarizability, $\alpha_{\alpha\beta}(\omega)$ by an analogous expression

$$\langle r_\alpha r_\beta\rangle_c = \frac{\hbar}{\pi}\int_0^\infty d\omega\,\alpha_{\alpha\beta}(i\omega), \quad (2.7)$$

which is sometimes referred to as the S_{-1} oscillator strength sum rule [35].

Using Eqs. (2.2) and (2.4) the second cumulant moment of the position operator can also be written as

$$\langle\hat{r}_\alpha\hat{r}_\beta\rangle_c = \iint d\boldsymbol{r}d\boldsymbol{r}'r_\alpha r'_\beta\{\rho(\boldsymbol{r})\delta(\boldsymbol{r} - \boldsymbol{r}') + \rho(\boldsymbol{r})h_{xc}(\boldsymbol{r},\boldsymbol{r}')\},$$
$$(2.8)$$

which shows that this quantity is the sum of a positive contribution, equal to the classical second moment of the charge distribution, $\rho(\boldsymbol{r})$, and an essentially nonclassical term which is due to the presence of correlations of Fermi and Coulomb type.

To analyze further the definition of $\langle\hat{r}_\alpha\hat{r}_\beta\rangle_c$, it will be useful to introduce the first and second moments of the xc-hole, expressed in the laboratory-frame:

$$D_\alpha^{xc}(\boldsymbol{r}) = -\int d\boldsymbol{r}'r'_\alpha h_{xc}(\boldsymbol{r},\boldsymbol{r}'), \quad (2.9)$$

$$Q_{\alpha\beta}^{xc}(\boldsymbol{r}) = -\int d\boldsymbol{r}'r'_\alpha r'_\beta h_{xc}(\boldsymbol{r},\boldsymbol{r}'). \quad (2.10)$$

Since $h_{xc}(\boldsymbol{r},\boldsymbol{r}')$ is a distribution normalized to -1, $D_\alpha^{xc}(\boldsymbol{r})$ can be regarded as component of the position vector of the xc-hole barycenter, i.e., the center

where the dipole moment of the xc-hole distribution $h_{xc}(\boldsymbol{r}, \boldsymbol{r}')$ for fixed $\boldsymbol{r}$ vanishes. According to the charge density reconstitution sum rule [36], which holds for the xc-hole (and also for the x-hole of single determinant wave functions) the total electronic moments μ_α and $\Theta_{\alpha\beta}$, can be obtained by taking the density weighted averages of the xc-hole moments:

$$\mu_\alpha = \int d\boldsymbol{r}\,\rho(\boldsymbol{r})D_\alpha^{xc}(\boldsymbol{r}), \qquad (2.11)$$

$$\Theta_{\alpha\beta} = \int d\boldsymbol{r}\,\rho(\boldsymbol{r})Q_{\alpha\beta}^{xc}(\boldsymbol{r}). \qquad (2.12)$$

Furthermore, the distance vector $\boldsymbol{d}(\boldsymbol{r})$ between the reference electron at position $\boldsymbol{r}$ and the barycenter of its xc-hole, $\boldsymbol{D}^{xc}(\boldsymbol{r})$, is introduced as

$$\boldsymbol{d}(\boldsymbol{r}) = \boldsymbol{D}^{xc}(\boldsymbol{r}) - \boldsymbol{r}. \qquad (2.13)$$

Following Becke and Johnson [37], this quantity can also be considered as the dipole of an electron-hole pair and, by consequence, it has been called the xc-hole dipole moment. Remark, that $\boldsymbol{d}(\boldsymbol{r})$ is a function of the position $\boldsymbol{r}$ of the reference electron.

From Eqs. (2.8) and (2.9) the second cumulant of the position operator can be expressed in terms of the xc-hole barycenter as

$$\langle \hat{r}_\alpha \hat{r}_\beta \rangle_c = \int d\boldsymbol{r}\,\rho(\boldsymbol{r})\{r_\alpha r_\beta - r_\alpha D_\beta^{xc}(\boldsymbol{r})\}. \qquad (2.14)$$

An equivalent, but more symmetrical expression, which makes obvious the origin-independence of the second cumulant moment, can be obtained by using the charge conservation sum-rule and the symmetry of the form-factor, either in terms of the form-factor itself,

$$\langle \hat{r}_\alpha \hat{r}_\beta \rangle_c = -\frac{1}{2}\int d\boldsymbol{r}\int d\boldsymbol{r}'(r - r')_\alpha(r - r')_\beta S(\boldsymbol{r}, \boldsymbol{r}'), \qquad (2.15)$$

or using the exchange-correlation hole, as

$$\langle \hat{r}_\alpha \hat{r}_\beta \rangle_c = -\frac{1}{2}\int d\boldsymbol{r}\,\rho(\boldsymbol{r})\int d\boldsymbol{r}'(r - r')_\alpha(r - r')_\beta h_{xc}(\boldsymbol{r}, \boldsymbol{r}'). \qquad (2.16)$$

Inspection of the second integral suggests that the second cumulant moment is proportional to the density-weighted average of the second moment of the xc-hole. By the virtue of the normalization of the xc-hole, and the definition of the xc-hole barycenter, Eq. (2.16) can be expanded as

$$\langle \hat{r}_\alpha \hat{r}_\beta \rangle_c = \frac{1}{2}\int d\boldsymbol{r}\,\rho(\boldsymbol{r})\{r_\alpha r_\beta - r_\alpha D_\beta^{xc}(\boldsymbol{r})$$
$$- D_\alpha^{xc}(\boldsymbol{r})r_\beta + Q_{\alpha\beta}^{xc}(\boldsymbol{r})\}. \qquad (2.17)$$

As a consequence of the charge-density reconstitution sum rule, the integrals of the last and first terms in curly brackets are equal to each other, both yielding the second moment of the charge density. Similarly the density weighted integrals of the sum of the two middle terms in the curly brackets are equal to the second contribution to (2.8). Although the definitions Eqs. (2.8) and (2.16) are equivalent, the integrands, in particular, i.e., the local functions in curly brackets, are different. In particular, while the expression in curly brackets in Eq. (2.8) is origin-dependent, the corresponding integrand in Eq. (2.17) is invariant. Therefore, it is only this latter form which may serve as starting point for the tentative construction of local measures of electron localization, as will be discussed in the following section.

3. Pointwise Measures of Electron Localization

In contrast to the localization tensor which provides a global measure of the nature of electrons, one expects from a local measure of localizability to characterize the spatial distribution of the itinerant or nonitinerant character of electrons. Strongly localized and delocalized groups of electrons may coexist in the same solid or molecular material and therefore it is of some interest to distinguish clearly such domains within the same system. As mentioned in the Introduction, various methods exist in the literature to construct electron localization functions, which accomplish this task with a certain success, but none of them has been related in an unequivocal manner to the localization tensor of Resta. In view of the clear physical meaning of the localization tensor as a global measure of the spontaneous dipolar fluctuations of the electron density and thereby related to their mobility under external perturbation, it is natural to seek for a quantity which is able to provide analogous information in a pointwise manner.

Looking at the definition of the trace of the second cumulant moment, a positive scalar quantity, the frame-independent integrand in Eq. (2.16) seems to be a possible candidate as a local measure of the electron localization. The function

$$\vartheta(\boldsymbol{r}) = -\frac{1}{2}\rho(\boldsymbol{r})\int d\boldsymbol{r}'(\boldsymbol{r} - \boldsymbol{r}') \cdot (\boldsymbol{r} - \boldsymbol{r}')h_{xc}(\boldsymbol{r}, \boldsymbol{r}') \qquad (3.1)$$

integrates to the global second cumulant and it can be interpreted as the density-weighted trace of the second moment of the exchange-correlation hole, $h_{\text{xc}}(\boldsymbol{r}, \boldsymbol{r}')$, measured with respect to the reference position, $\boldsymbol{r}$ of the electron. Using the xc-hole barycenter vector, $\boldsymbol{D}^{\text{xc}}(\boldsymbol{r})$, the xc-hole dipole, $\boldsymbol{d}(\boldsymbol{r})$ as well as the trace of the second xc-hole moment $Q^{\text{xc}}(\boldsymbol{r})$, one obtains the following compact expression for $\vartheta(\boldsymbol{r})$:

$$\vartheta(\boldsymbol{r}) = \frac{1}{2}\rho(\boldsymbol{r})\{Q(\boldsymbol{r}) - \boldsymbol{D}(\boldsymbol{r}) \cdot \boldsymbol{D}(\boldsymbol{r}) + \boldsymbol{d}(\boldsymbol{r}) \cdot \boldsymbol{d}(\boldsymbol{r})\}. \quad (3.2)$$

Since the second moment of a distribution is related to its spatial extent, a diffuse hole with large second moment can be naturally associated with a delocalized electron, while on the contrary, a compact hole with a small second moment can be considered as typical for a strongly localized electron. However, the above tentative definition has an obvious shortcoming: the second moment of a distribution with nonzero charge, that of the xc-hole, depends on the choice of the origin, $\boldsymbol{r}$. This origin-dependence has the undesirable effect that for reference points within the same localization domain, where the shape of the xc-hole is supposed to be approximately constant, the approximate constancy of the second moment is not necessarily maintained. For instance, $\vartheta(\boldsymbol{r})$ will be expected to be small near the centroid of the localization domain and to increase with increasing distance of the reference point with respect to the xc-hole barycenter.

The undesirable origin dependence can be avoided by modifying the local function and choosing the origin for measuring the second moment of the xc-hole as the barycenter of the xc-hole itself, $\boldsymbol{D}(\boldsymbol{r})$. This quantity, called $\kappa(\boldsymbol{r})$ is expected to measure the intrinsic second moment of the xc-hole:

$$\kappa(\boldsymbol{r}) = -\frac{1}{2}\rho(\boldsymbol{r})\int d\boldsymbol{r}'(\boldsymbol{D}(\boldsymbol{r}) - \boldsymbol{r}') \cdot (\boldsymbol{D}(\boldsymbol{r}) - \boldsymbol{r}')h_{\text{xc}}(\boldsymbol{r}, \boldsymbol{r}')$$
$$= \frac{1}{2}\rho(\boldsymbol{r})\{Q(\boldsymbol{r}) - \boldsymbol{D}(\boldsymbol{r}) \cdot \boldsymbol{D}(\boldsymbol{r})\}. \quad (3.3)$$

Although $\kappa(\boldsymbol{r})$ does not integrate to the second cumulant moment, it might be an appropriate candidate as a function to characterize the spatial extent of the xc-hole and by consequence the localized or delocalized nature of electrons.

The difference between $\vartheta(\boldsymbol{r})$ and $\kappa(\boldsymbol{r})$,

$$\vartheta(\boldsymbol{r}) - \kappa(\boldsymbol{r}) = \frac{1}{2}\xi(\boldsymbol{r}) = \frac{1}{2}\rho(\boldsymbol{r})\boldsymbol{d}(\boldsymbol{r}) \cdot \boldsymbol{d}(\boldsymbol{r}), \quad (3.4)$$

defines a function, $\xi(\boldsymbol{r})$, which integrates to the density-weighted squared xc-hole dipole moment

$$\langle d^2 \rangle = \int d\boldsymbol{r}\,\xi(\boldsymbol{r}) = \int d\boldsymbol{r}\,\rho(\boldsymbol{r})d^2(\boldsymbol{r}). \quad (3.5)$$

The quantities $d^2(\boldsymbol{r})$ and $\langle d^2 \rangle$ have appeared in the literature recently in the context of the heuristic model for the van der Waals forces by Becke and Johnson [37]. According to these authors, $\langle d^2 \rangle$ can be considered as an approximation to the second cumulant moment, $\langle r^2 \rangle_c$. Although the status of the function $\xi(\boldsymbol{r})$ and the meaning of its integral taken over the whole space is far from being fully understood [38, 39], this function arises quite naturally as a possible further candidate to characterize localization. As a tentative interpretation of its physical meaning, one may recall that in geometrical terms $\boldsymbol{D}^{\text{xc}}(\boldsymbol{r}) - \boldsymbol{r}$ is the vector connecting the position of the electron to the barycenter of its xc-hole. In this sense $d^2(\boldsymbol{r})$ measures the "locality" of the xc-hole, and it may be judicious to call it as Fermi-hole locality indicator (FHLI).

4. Results

All the three suggested functions are positive and bound from below by 0, while they are in principle unbounded from above. To have a unique scale, these function have been mapped on the interval [0:1] by the transformation $(1 + f(\boldsymbol{r}))^{-1}$ and numerically tested for a set of molecules. It turned out that only the quantity derived from $\xi(\boldsymbol{r})$ is able to display chemically meaningful details; the two other local functions provide relatively boring and structureless pictures about the organization of electrons.

In the following, $(1 + \xi(\boldsymbol{r}))^{-1}$, the Fermi-hole locality indicator (FHLI) will be applied to a selection of simple molecules, spanning a range of different bonding situations. The forthcoming numerical illustrations will be restricted to single-determinant wave functions, where the correlation hole is vanishing and the above-defined quantities will be calculated exclusively from the exchange hole. Since the main purpose of these illustrations is to provide a qualitative overview, all examples were calculated at standard geometries at the RHF/6-311G** level. The necessary formulae were implemented in a development version of the Molpro 2008.2 quantum chemical package [40]. Regular grids with 0.125 bohr stepsize (for a few larger systems with step of 0.15 bohr) were generated in the standard cube format.

The same regular grids were used to perform approximate numerical integration of the various characteristic functions leading to the second cumulant moment, the average of the squared

TABLE I

Trace of the localization tensor for a set of simple molecules calculated at the RHF/6-311G** level and the results of numerical integration on a simple regular grid of the functions $\vartheta(\boldsymbol{r})$, $\xi(\boldsymbol{r})$, and $\int \kappa(\boldsymbol{r})$.

Compound	λ	$\int \vartheta(\boldsymbol{r})/N$	$\int \xi(\boldsymbol{r})/N$	$\int \kappa(\boldsymbol{r})/N$
B_2H_6	2.1485	2.15	1.37	1.46
C_4H_4	1.9412	1.94	1.02	1.43
CH_4	1.8960	1.90	1.31	1.24
C_4H_6	1.8660	1.86	1.02	1.35
C_6H_6	1.8599	1.86	0.88	1.42
C_2H_4	1.8510	1.85	1.14	1.28
C_2H_6	1.8400	1.84	1.14	1.27
C_2H_2	1.8202	1.82	1.16	1.24
NH_3	1.5657	1.56	1.11	1.01
CS_2	1.5537	1.55	0.83	1.13
H_2CO	1.3840	1.38	0.86	0.95
N_2	1.3389	1.34	0.82	0.93
$ClNO$	1.2983	1.29	0.71	0.94
CO	1.2609	1.26	0.80	0.86
H_2O	1.1791	1.18	0.84	0.76
He	1.1765	1.16	1.18	0.57
Ar	0.9105	0.91	0.63	0.60
F_2	0.8470	0.85	0.50	0.60
SF_6	0.8250	0.82	0.39	0.63
Ne	0.5855	0.58	0.41	0.38

C_4H_4 corresponds to $CH_2=C=C=CH_2$, C_4H_6 to $CH_2-CH=CH-CH_2$.

exchange-hole dipole moment, and the average trace of the intrinsic exchange-hole second moment (cf. Table I.) The precision of these integrations is roughly 10^{-3} to 10^{-2} as it can be seen by comparing the second cumulant moments calculated both by analytical and numerical integrations presented in the second and third columns of Table I. The global characteristic values are displayed normalized by the number of electrons for each system. The atoms and molecules are presented in the order of the decreasing value of $\lambda = \langle \hat{r}^2 \rangle_c /N$. It is remarkable that the average trace of the x-hole second moment follows essentially the same ordering as λ, while there are considerably more exceptions for the average of the squared x-hole dipole moments. The relationship (3.4) is verified by the calculated values. The highest degree of delocalized character is shown by the nonclassical diborane with its multicenter bonds, while the most localized species in this collection are the rare gas atoms and the SF_6 molecule.

Molecular structures and isosurfaces generated from the cube files were displayed using the VMD 1.8.6 molecular graphics package. Figure 1 shows

the case of carbon–carbon single, double, and triple bonds on the examples of ethane, ethylene, and acetylene. The isosurface value has been chosen as 0.91 for the ethane and ethylene, while, to observe more details, a slightly higher value, 0.925 was used for acetylene. The C–C sigma bond is characterized by a pair of maxima developed on the bond axis near to the two bonded atoms. Similar structures appear at higher isosurface values on the C–H bonds as well. The C=C double bond can be identified by a pair of domains, resembling strongly distorted p-orbitals, which will join each other at higher isosurface values. The triple bond of acetylene gives rise to a pair of characteristic disk-like structures situated near the carbon atoms.

The N_2 and CO molecules (Fig. 2) are isoelectronic with the acetylene. The topological analogies of these systems are quite obvious, the main difference being that the electron pairs situated on the H atoms and the H–C bonds are now lone pairs, which form a kind of crown in N_2 (at least at the isosurface of 0.901) which becomes a form of mushroom at slightly higher values of the isosurface. Essentially the same structure appears in the case of CO, but strongly distorted toward the more electronegative oxygen atom.

A further isoelectronic series is represented by the group of molecules CH_4, NH_3, and H_2O (Fig. 3). A small maximum can be observed near the central atom on the X–H bonds. The extension of the lone pair lobes correlates well with the known variation of the bond angles in agreement with the VSEPR model of Gillespie.

Finally, Figure 4 presents three interesting bonding situations. The case benzene illustrates quite well the presence of a continuous path formed under and above the aromatic ring. This structure resembles strongly to the double-bond shapes, the only difference being that the "heads" of the distorted p-orbital-like lobes are touching each other. The picture of the SF_6 molecule is dominated by the "mushrooms" of the fluorine lone pairs. The S–F bonds are characterized by a pair of tiny and dissymmetric maxima along the interatomic axis. This molecule happens to be the more localized according to the global localization tensor measure, indicating that the bonding is most probably strongly ionic. The diborane molecule, identified as the most "delocalized" systems of all the examples selected in this study, shows some reminiscence to the ethylene: the p-orbital-like structures are highly deformed and show a strong concentration above and below the plane of the equatorial H atoms.
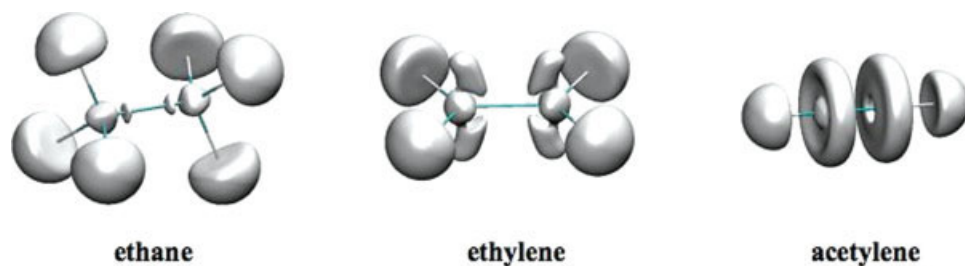
FIGURE 1. FHLI isosurfaces for ethane ($\xi = 0.91$), ethylene ($\xi = 0.91$), and acetylene ($\xi = 0.925$). [Color figure can be viewed in the online issue, which is available at www.interscience.wiley.com.]

FIGURE 2. FHLI isosurfaces for dinitrogen ($\xi = 0.901$) and carbon monoxide ($\xi = 0.925$). [Color figure can be viewed in the online issue, which is available at www.interscience.wiley.com.]
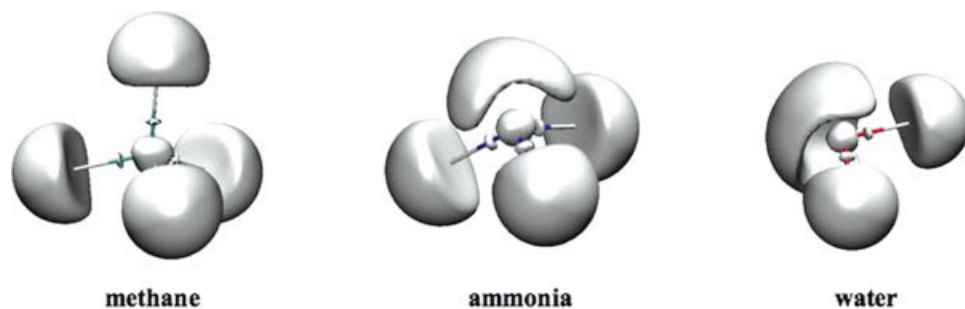

FIGURE 3. FHLI isosurfaces for methane ($\xi = 0.92$), ammonia ($\xi = 0.915$), and water ($\xi = 0.925$). [Color figure can be viewed in the online issue, which is available at www.interscience.wiley.com.]
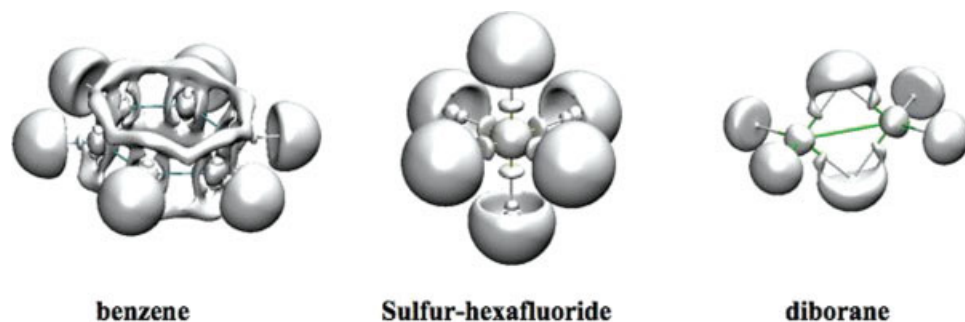

FIGURE 4. FHLI isosurfaces for benzene ($\xi = 0.93$), sulfur-hexafluoride ($\xi = 0.91$), and diborane ($\xi = 0.91$). [Color figure can be viewed in the online issue, which is available at www.interscience.wiley.com.]

As compared to the corresponding ELF isosurfaces, the observed similarities in a few cases are striking. However, there are some significant differences, of which the most important is that the number of attractors (analyzed for the time being by inspection) does not correspond always to those of the ELF.

5. Conclusions and Perspectives

It has been found that neither the frame-invariant integrand that arises in the calculation of the second cumulant moment of the position operator nor the intrinsic exchange hole second moment, constructed as to measure the second moment with respect to the centroid of the x-hole, can serve a meaningful local indicator of the electrons pair organization in many-electron systems. On the other hand, the density-weighted square of the x-hole dipole moment, tentatively named Fermi-hole locality indicator (FHLI) may be useful to reveal details about the spatial distribution of electron localization. Although this quantity does not integrate to Resta's localization tensor, it is closely related to it. Further research is needed to analyze the topological properties of the FHLI and see if it were able to provide deeper or different insight as compared to other local measures of electron localization. Based on a limited number of examples presented here, and also on the basis of a set of further unpublished cases, the FHLI, just like ELF, is able to rationalize the predictions of the VSEPR model of chemical structure of bonding in terms of simple and suggestive graphical representations, based on a function derived from the many-electron wave function.

Independently of the future usage of FHLI for interpretation purposes, a visual inspection of the $\xi(\mathbf{r})$ function is interesting also from the perspective of its application in the heuristic dispersion force model of Becke and Johnson. The fact that the strongest maxima of $\xi(\mathbf{r})$ seem to be located near the atomic centers supports the strategy of using atomic averages of $\langle d^2 \rangle$ in setting up dispersion force models.

References

1. Bader, R. W. F. Atoms in Molecules—A Quantum Theory; University of Oxford Press: Oxford, 1990.
2. Resta, R. J Phys Condens Matter 2002, 14, R625.
3. Resta, R. J Chem Phys 2006, 124, 104104.
4. Kohn, W. Phys Rev 1964, 133, 171.
5. Chalvet, O.; Daudel, R.; Diner, S.; Malrieu, J. P., Eds. Localization and Delocalization in Quantum Chemistry, vol. I–II. Reidel: Dordrecht, 1975.
6. Resta, R.; Sorella, S. Phys Rev Lett 1999, 82, 370.
7. Boys, S. F. Rev Mod Phys 1960, 32, 296.
8. Boys, S. F. In Quantum Theory of Atoms, Molecules and Solid State: A Tribute to John C. Slater; Löwdin, P.-O., Ed.; Academic Press: New York, 1966; p 253.
9. Becke, A. D.; Edgecombe, K. E. J Chem Phys 1990, 92, 5397.
10. Dobson, J. F. J Chem Phys 1991, 94, 4328.
11. Savin, A.; Becke, A. D.; Flad, J.; Nesper, R.; Preuss, H.; von Schnering, H. G. Angew Chem Int Ed Engl 1991, 30, 409.
12. Poater, J.; Duran, M.; Solà, M.; Silvi, B. Chem Rev 2005, 105, 3911.
13. Silvi, B.; Savin, A. Nature 1994, 371, 683.
14. Silvi, B. J Phys Chem A 2003, 107, 3081.
15. Kohout, M. Int J Quantum Chem 2004, 97, 651.
16. Kohout, M. Faraday Discuss 2007, 135, 43.
17. Schmider, H. L.; Becke, A. D. J Chem Phys 2002, 116, 3184.
18. Geier, J. J Phys Chem A 2008, 112, 5187.
19. Hirschfeld, F. L. Theor Chim Acta 1977, 44, 129.
20. Mayer, I. Simple Theorems, Proofs and Derivations in Quantum Chemistry; Kluwer: New York, 2003.
21. Mayer, I. J Comput Chem 2007, 28, 204.
22. Ángyán, J. G. J Mol Struct (Theochem) 2000, 501–502, 379.
23. Stone, A. J. Mol Phys 1985, 56, 1065.
24. Ángyán, J. G.; Jansen, G.; Loos, M.; Hättig, C.; Hess, B. A. Chem Phys Lett 1994, 219, 267.
25. Ángyán, J. G.; Loos, M.; Mayer, I. J Phys Chem 1994, 98, 5244.
26. Mayer, I. Theor Chim Acta 1985, 67, 315.
27. Mayer, I. Chem Phys Lett 1983, 97, 270.
28. Fradera, X.; Austen, M. A.; Bader, R. F. W. J Phys Chem A 1999, 103, 304.
29. Ponec, R.; Cooper, D. L. J Mol Struct (Theochem) 2005, 727, 133.
30. Luken, W. L. In The Concept of the Chemical Bond; Maksic, Z., Ed.; Springer Verlag: Berlin, 1990; vol. 2, p 287.
31. Ponec, R.; Cooper, D. L. J Phys Chem A 2007, 111, 11294 .
32. Ayers, P. W. J Chem Sci 2005, 117, 441.
33. Ziesche, P. J Mol Struct (Theochem) 2000, 527, 35.
34. Langreth, D. C.; Perdew, J. C. Phys Rev B 1977, 15, 2884.
35. Hirschfelder, J. O.; Brown, W. B.; Epstein, S. T. Adv Quantum Chem 1964, 1, 255.
36. Gori-Giorgi, P. Ángyán, J. G.; Savin, A. Can J Chem (in press).
37. Becke, A. D.; Johnson, E. R. J Chem Phys 2005, 122, 154104.
38. Ángyán, J. G. J Chem Phys 2007, 127, 024108.
39. Ayers, P. W. J Math Chem, DOI 10.1007/s10910-008-9451-y (in press).
40. Werner, H.-J.; Knowles, P. J.; Lindh, R.; Manby, F. R.; Schütz, M.; Celani, P.; Korona, T.; Mitrushenkov, A.; Rauhut, G.; Adler, T. B.; Amos, R. D.; Bernhardsson, A.; Berning, A.; Cooper, D. L.; Deegan, M. J. O.; Dobbyn, A. J.; Eckert, F.; Goll, E.; Hampel, C.; Hetzer, G.; Hrenar, T.; Knizia, G.; Köppl, C.; Liu, Y.; Lloyd, A. W.; Mata, R. A.; May, A. J.; McNicholas, S. J.; Meyer, W.; Mura, M. E.; Nicklass, A.; Palmieri, P.; Pflüger, K.; Pitzer, R.; Reiher, M.; Schumann, U.; Stoll, H.; Stone, A. J.; Tarroni, R.; Thorsteinsson, T.; Wang, M.; Wolf, A. Molpro, version 2008.2, a package of ab initio programs. Available at: http://www.molpro.net.